Formulation of zeolite supported nano-metallic catalyst and applications in textile effluent treatment

Tazien Rashid[a], Danish Iqbal[b], Abu Hazafa[c], Sadiq Hussain[b], Falak Sher[d], Farooq Sher[e,*]

a. Department of Chemical Engineering, Universiti Teknologi Petronas, Bandar Seri Iskandar, Tronoh 32610, Perak, Malaysia
b. Department of Chemical Engineering NFC Institute of Engineering and Technology, Multan, Pakistan
c. Department of Biochemistry, University of Agriculture, Faisalabad, 38000, Pakistan
d. Department of Chemistry and Chemical Engineering, Syed Babar Ali School of Science and Engineering, Lahore University of Management Sciences (LUMS), Lahore, Pakistan
e. School of Mechanical, Aerospace and Automotive Engineering, Faculty of Engineering, Environmental and Computing, Coventry University, Coventry CV1 5EB, UK

[*] Corresponding author:
Email: Farooq.Sher@coventry.ac.uk; Tel: +44 (0) 24 7765 7688

Highlights

- The borohydride method was used to synthesize a novel natural zeolite-supported nano-zerovalent iron (NZ-nZVI) catalyst.
- The unprocessed naturally mined zeolite was used as support for nZVI to decrease the aggregation and cost.
- The synthetic acid orange 52 dye was removed over 94.86% after 180 min treatment with novel natural zeolite modified nZVI.
- More than 60% of dye removal was observed within the first 10 min of treatment with NZ-nZVI at 15 mg/L concentration.
- NZ-nZVI/SPC Fenton system also effectively removed the green, magenta, and blended colour from the actual textile effluents.

Abstract

Textile industry is one of the major industries worldwide and produces a huge amount of coloured effluents. The presence of coloured compounds (dyes) in water change its aesthetic value and cause serious health and environmental consequences. However, the present investigation was carried out to minimize and reduce the colour compounds discharged by the textile industries through a nano-scaled catalyst. This study is mainly focused on the explanation of nanoparticles aggregation by deposition on natural zeolite, and utilization of this natural zeolite as supported material to nano zerovalent iron (NZ-nZVI) in the form of liquid slurry with sodium percarbonate acting as an oxidant in a Fenton like system for the removal of synthetic CI acid orange 52 (AO52) azo dye, in textile effluent. The nano-scaled zerovalent irons were synthesized by borohydride method in ethanolic medium. UV-vis spectrophotometry, FTIR, EDX, SEM, and XRD (powdered) analysis were used for the investigations of surface morphology, composition, and properties of natural zeolite supported nZVI and study the dye removal mechanism. The XRD spectrum revealed that clinoptilolite is the major component of natural zeolite used, while EDX found that the iron content of NZ-nZVI was about 9.5%. The introduction of natural zeolite as supporting material in the formation of iron nanoparticle resulted in the partial reduction of aggregation of zerovalent iron nanoparticles. The findings revealed that the 94.86% removal of CI acid orange 52 dye was obtained after 180 min treatment at 15 mg/L initial dye concentration. The highest rapid dye removal of about 60% was achieved within the first 10 min of treatment at the same dye concentration. Furthermore, the actual dyeing effluent including green, magenta, and the blended colour was successfully decolourized by natural zeolite-supported nZVI/SPC Fenton process. It is concluded that the acceleration of corrosion of NZ-nZVI, breaking of azo bond, and consumption of Fe^{2+} were the possible mechanisms behind the removal of AO52 dye. It is also recommended

that NZ-nZVI/SPC Fenton process could be a viable option for effluent and groundwater remediation.

Keywords: Fenton process; Natural zeolite; nano zerovalent iron; CI acid orange 52 dye; dye removal; and Textile dyeing wastewater.

1 Introduction

The textile industry is one of the major industries worldwide and the highest consumer of raw water. This sector is growing proportionally with an increasing demand for textile products worldwide. This increase is also causing an increase in water demand and consequently increased effluent discharge [1, 2]. The major operations involved in the textile industry are spinning (twisting of fibres to form thread), weaving (arranging two different sets of threads perpendicular to each other to form fabric), and finishing. Finishing steps might contain several elements, including washing, bleaching, stabilizing and dyeing operations [3]. The inappropriate discarding of industrial wastes including dyes causes serious health and environmental problems [4]. According to accumulated data, worldwide there is 7–10 million ton annual dye production and commercially more than one million types of dyes exist [1]. In this total dye production >2.8 million tons of textile dyes are discharged as industrial wastes [5]. Dyes are usually classified according to their usage and application method. Among all dyes including reactive, direct, vat, disperse, azo, acid and anthraquinone dyes, the azo dye holds up to 70% market share of all organic dyes [6-8].

Major constituents of textile effluent are colour, total dissolved solids (TDS), chemical oxygen demand (COD), turbidity, and pH. The presence of dyes in the effluent affects the aesthetic value

of the water and possesses severe environmental and health threats. They tend to adversely affect aquatic life and are carcinogenic for human beings [9]. Several prominent azo dyes are degradable into amines in an intestinal environment, which are proven carcinogens [10]. Carcinogenic threats are not only limited to azo family dyes. The anthraquinone dyes, such as Disperse Blue 3 is also found to have severe toxic effects [11, 12]. The removal of colouring ingredients from the wastewater poses a major challenge. According to current industrial practices, different methods are being applied for the removal of dyes from wastewater, including physical (powdered/granulated activated carbon and adsorption), chemical (coagulation), and biological (fungal decolourization or microbial degradation). However, due to low biodegradability, high cost, low efficiency and toxic byproducts (DBPs), these methods attain less attention [9, 13, 14]. The advanced oxidation process (AOP) is an alternative method for the removal of dyes from industrial effluent [15].

The advanced oxidation process (AOP) relies on the oxidation of organic contaminants by involving highly reactive species such as hydroxyl radical (OH), hydrogen peroxide (H_2O_2), ozone (O_3) and sulfate radical ($SO^{4\,-}$), for the removal of dyes. Furthermore, AOP has the potential to offer complete or satisfactory degradation of textile dyes and other contaminants, unlike other conventional methods [9, 16]. AOP includes Fenton process, per-ozonation, H_2O_2/UV, photo-Fenton, O_3/UV, and Sono-AOP. Due to high reactivity and efficient remediation of contaminants, the Fenton process is being focused upon as AOP of choice among all processes. Fenton process includes disintegration of hydrogen peroxide (H_2O_2) by ferrous ion (Fe^{2+}) to generate hydroxyl radical which further binds with organic impurities to remove dyes/colour from water according to following Eqs. (1–3) [17, 18]. In the last few decades, many heterogeneous catalysts including

Fe_2O_3, Ag_2O, ZnO, and TiO_2 have been used to depollute water from toxic metal ions (Cr^{VI}) and other pollutants like dyes [19, 20].

$$Fe^0 + 2H^+ \rightarrow Fe^{2+} + H_2 \quad (1)$$

$$Fe^0 + H_2O_2 + 2H^+ \rightarrow Fe^{2+} + 2H_2O \quad (2)$$

$$Fe^{2+} + H_2O_2 \rightarrow Fe^{3+} + OH^- + O\dot{H} \quad (3)$$

The nanotechnology for dye removal has achieved special attention in the scientific community since the last decade. Nano-zerovalent iron (nZVI) got more focus due to superior dye removal efficiency, less toxicity, and cost-effective characteristics. nZVI particles have less than 100 nm size, due to their smaller particle size; they possess higher surface area (29 m^2/g) and display higher reactivity than mZVI (micro nano-zerovalent iron). Due to its high surface area, it can be effectively used as an adsorbent for textile dye removal [21]. According to previously published literature, more than 90% of decolourization of methyl orange dye was observed with nZVI in 24 min treatment while only 25% of decolourization was achieved by mZVI with the same treatment time [22]. Use of hydrogen peroxide can be difficult due to transportation, storage and usage challenges. Recently, sodium percarbonate has been suggested as a novel source of H_2O_2. It contains hydrogen peroxide within its matrix, which it releases on dissolution in water by the following Eq. (4) [17, 18].

$$2Na_2CO_3.3H_2O_2 \rightarrow 2Na_2CO_3 + 3H_2O_2 \quad (4)$$

nZVI particles tend to aggregate due to their magnetic properties and Van der Waals attraction. This is one of the two major inhibitors of nZVI's performance, the other being their rapid corrosion on exposure to air. Aggregation of nZVI depends upon particle concentration, size of particles, magnetic properties, surface area to volume ratio and pH [23]. Recently several support materials

have been used as good carriers to decrease the aggregation of nZVI including alumina, chitosan, bentonite, graphene oxide, biochar, coral, kaolin, clinoptilolite, and activated carbon [24, 25].

In the previously published literature less reactive, high price and toxic by-products of these supporting materials have been observed. Therefore, for the first time, the natural zeolite (due to its high cation exchange capacity) as support material with nZVI to decrease its aggregation, enhance biodegradability and efficiency to remove synthetic and textile dyes is used in the present study. Shi and co-workers [26] reported the 86.4% removal of Rhodamine B dye within 20 min by using nZVI particles with reduced graphene oxide (r-GO) as a supported carrier. They also observed nanoparticles dispersion on the graphene oxide sheet with decreased aggregation. However, some aggregation persisted even after the deposition of nZVI upon the r-GO sheet. Han and his research group [27] used biochar as support material for nZVI in the removal process of methyl orange dye. They observed an improved dispersion and reactivity of nanoparticles, as well as enhanced adsorption capacity resulting in 98.5% dye removal at a composite dose of as low as 600 mg/L, at an optimum pH of 4 within 10 min. Jin and co-workers [28] suggested the use of nZVI and kaolin in equal mass ratios, in a removal study of Direct Fast Black G dye and reported 99.8% removal of dye in 1 h even in the alkaline range of 9.4.

Another study found bentonite as a better option (92.7% dye removal) than native clay (92.1%) and kaoline (91.6%) for remediation of an industrial azo dye [29]. Malik and co-workers reported that nZVI, Fe and ozone pre-treatment on actual filtrated textile effluent showed significant results of about 0.61 for biochemical and chemical oxygen demands (BOD/COD) with 87% of colour removal, as compared to untreated effluent [30]. Similarly, ultrasonication supported the removal

of toxic Remazol black 133 dye up to 80% within 15 min treatment at an optimum pH range of 4–10. They also noticed that one gram of nZVI removed approximately 749 mg of dye, by breaking the azo group into an amino group. They also suggested that dye removal efficiency was increased via increasing nanoparticles dosage [31]. Luo and coworkers demonstrated a complete removal of orange II dye using rectorite (a natural clay), as support for nZVI in 10 min treatment, while only 35% dye removal was observed by using unsupported nZVI [32].

However, many supporting materials (kaolin, bentonite, biochar, alumina, and chitosan) have been applied in combination with nZVI to decrease its aggregation and increase reactivity, but the above-mentioned supported materials are expensive and produce toxic by-products like DBPs. To overcome this problem, for the first time, this study investigates the synthesis of natural zeolite as supported material of nano-zerovalent iron (NZ-nZVI) by using borohydride method to remove the synthetic dye (CI Acid Orange 52) from textile waste. SEM, EDX, FTIR and UV/VIS analyses were performed to evaluate the structure and performance of natural zeolite and synthesized NZ-nZVI. Furthermore, present study also assessed the mutagenic dye remediation potential of NZ-nZVI in a Fenton like process by using sodium percarbonate (SPC) as a source of reactive advance oxidative species for both synthetic dye solution and actual textile effluents. To deal with the corrosion of nZVI on exposure to ambient air, nZVI was synthesized and introduced to target solution in the form of a liquid slurry.

2 Materials and methods

2.1 Chemicals

Sodium Borohydride ($NaBH_4$: 97%) was procured from Deajung, Korea. Iron (II) Sulphate Heptahydrate ($FeSO_4.7H_2O$) and Ethanol (Absolute) were purchased from BDH. Natural Zeolite

was procured from Meiqi Trade Co. China. Sulfuric Acid (H_2SO_4), Sodium Percarbonate ($Na_2CO_3.1.5H_2O_2$) and Sodium Hydroxide (NaOH) were purchased from Sigma Aldrich (USA). CI Acid Orange 52 (methyl orange) dye was purchased from Sinochem, China. Actual dyeing effluent was obtained from Multan Yarn Dyeing, located at home-tex export zone, Multan, Pakistan.

2.2 Preparation of NZ-nZVI catalyst

NZ-nZVI was synthesized by borohydride method, also known as reduction method, or liquid phase reduction method according to the following Eq. (5) [33, 34]:

$$Fe^{2+} + 2BH_4^- + 6H_2O \rightarrow Fe^0 + 2B(OH)_3 + 7H_2 \uparrow \quad (5)$$

The preparation of NZ-nZVI was achieved by adding a 250 mL solution of ethanol in deionized water (40%) made in a Pyrex beaker. The solution of $FeSO_4.7H_2O$ was added into the ethanol-water mixture, it is readily soluble in water and dissolved immediately with mild stirring. Then the natural zeolite which is composed of clinoptilolite (85.7%), SiO_2 (65.5%), Al_2O_3 (12.3), Fe_2O_3 (1.49), CaO (3.97), MgO (0.92), and K_2O (1.54) [35] (pulverized and sieved < 63 µm) was added with the ratio of 1:2 of $FeSO_4.7H_2O$ and Zeolite. The pH was maintained at 4 and ultrasonicated for 15 min; the pH of $FeSO_4.7H_2O$ solution increased to around 5–5.5. To maintain the pH a few drops of H_2SO_4 solution (approx. 0.4 M) were added to decrease the pH to 4. The ultrasonication was used to breakdown iron sulfate agglomerates and effectively disperse the zeolite and iron sulfate in an aqueous matrix to improve the iron sulfate adsorption on the zeolite surface. The pH is a critical factor in the preparation of NZ-nZVI because as near neutral pH, the nZVI starts to precipitate in the aqueous solution in the form of iron oxides and hydroxides. After the homogenization of reaction mixture, 1 M $NaBH_4$ was added at a rate of 1.6–2 mL/min with

moderate stirring. The synthesis of nZVI on the support of natural zeolite (NZ) was achieved according to the following Eq. (6) [36].

$$2Fe^{2+}(aq) + BH_4^-(aq) + 2H_2O + \text{support} \rightarrow 2F^0/\text{support}\,(s) + BO_2^-(aq) + 4H^+(aq) + 2H_2(g) \quad (6)$$

NZ-nZVI particles are formed almost immediately, indicating an initiation of the reduction process. $NaBH_4$ gives off hydrogen gas in water, and hence its solution cannot be stocked. It must be prepared 10 min before use. If NZ-nZVI made immediately prior to use, the emitting hydrogen gas can cause heavy froth in the reaction mixture. The emitted hydrogen froth prevents the further addition of $NaBH_4$ and reduces the zeolite supported iron in the aqueous solution and form nZVI instead of NZ-nZVI. When the reduction of iron has completed, it was remained to settle down for 1 h and finally stored in the same reaction media. The nanoparticles must not be exposed to the ambient air in order to prevent the corrosion of iron. Literature also recommends the storage of nanoparticles in nitrogen environment to prevent rusting [36, 37].

2.3 Preparation of synthetic methyl orange dye and actual dying effluents

Dye removal studies were performed for both synthetic and actual textile effluent. Concentrated dye stock solution of CI Acid Orange 52 (methyl orange) was prepared with a concentration of 35 ppm and various solutions for removal studies were prepared by serial dilutions. The dye stock solution was prepared at least 24 h prior to use because some undissolved dye fragments remain in the solution even after 2–3 h of mixing and may need a longer time to completely dissolve. The preparation of dye was achieved by adding 250 mL of dye solution diluted up to the required concentration in a Pyrex beaker, which served as the reaction vessel [38]. 40 mL of NZ-nZVI slurry and sodium percarbonate was added into the reaction vessel and continuously stirred at 450

rpm. The synthetic dye solution was prepared by mixing Acid Orange 52 (AO52) dye, a bright orange powder, with distilled water. Initially, a 35 pm stock solution was prepared, which was then serially diluted to the required concentrations. The actual dyeing effluent was prepared by adding 250 mL of textile effluent sample in a Pyrex Erlenmeyer flask with deionized water. Erlenmeyer flask is recommended, as high froth generation could be observed in the treatment of low pH dye effluents. The NZ-nZVI slurry and sodium percarbonate (SPC) solution was added into the Erlenmeyer flask and stirred at 450 rpm.

2.4 Characterization of NZ-nZVI catalyst

The nano zerovalent iron particles supported on natural zeolite were analyzed by using FEI Quanta 250 scanning electron microscopy (SEM) for studying the surface morphology along with energy-dispersive X-ray spectroscopy, while the mineralogical content was studied using Malvern Panalytical X-pert Pro XRD. Elemental composition was detected to confirm the iron loading on natural zeolite by INCA X-Act Electron Back Scattered Diffraction System (Oxford Instruments, U.K). Removal of dye from target dye solutions was recorded by UV-vis Spectrophotometry (model V1100), while the functional groups found on the raw natural zeolite and NZ-nZVI were studied using Fourier transform infrared spectroscopy (Perken Elmers Spectrum: FTIR).

2.5 The percentage removal efficiency of CI Acid Orange 52 dye and actual dying effluent

Five different concentrations of synthetic dye solution (AO52) were synthesized as follows 5, 10, 15, 20, and 25 mg/L. UV-vis spectrophotometer was used to investigate the change in dye concentration concerning time and its work according to the Beer-Lambert law. Deviation from this law is observed on too high concentrations of analyte, possibly due to electrostatic interactions of molecules. Hence, to ensure the accuracy of absorbance measurement, dye concentration was

limited to 25 mg/L. AO52 solutions (250 mL) were stored in dark, to avoid any UV oxidation. Stirrer rpm, pH and temperature were kept constant during all runs. The dye (AO52) removal efficiency was reported over the course of 180 min. multiple absorbance of each sample were recorded at 465 nm, and the average value was reported.

In actual dyeing effluent, the dye removal study was performed on three samples as actual effluent green (AEG), actual effluent magenta (AEM), and actual effluent blended (50% AEG + 50% AEM = AEB). Samples were treated with NZ-nZVI/SPC system without any filtration or dilution. To the best of our knowledge, this is unprecedented in scientific literature, as actual samples are often diluted up to several times or passed through some polishing step prior to treatment. The dye removal efficiency was reported over the course of 180 min at natural pH of effluent [39]. IR and UV-vis absorbance spectra were used to understand the dye removal process. Periodically, approximately a 4 mL sample was taken, filtered to remove NZ-nZVI particles and then filled into the glass cuvette for absorption determination by UV-vis spectrophotometer. Absorption was measured against distilled water (in case of actual effluents) and 9 mM sodium percarbonate (SPC) solution (in case of AO52) as blanks. The removal efficiency was calculated by the following Eq. (7).

$$\%\,\text{removal} = (A_0 - A_t) \,/\, A_0 \times 100 \quad (7)$$

where A_0 represents the initial values of synthetic dye (AO52) and actual effluent (green, magenta, and blended) in mg/L, and A_t represents the values of synthetic dye and actual effluent at time t.

The heavy froth was observed by the addition of NZ-nZVI/SPC into the reaction vessel of actual dye. Which might be due to the maximum reactivity of Fenton system that occurs at acidic pH. Therefore, the Erlenmeyer flask is recommended to avoid any reagent loss by dropping froth out of the reaction vessel.

3 Results and discussion

3.1 Characterization study of NZ-nZVI

The characterization studies were performed by scanning electron microscope (SEM), X-ray diffraction (XRD), Fourier transform infrared spectroscopy (FTIR) and energy dispersive X-Ray (EDX) Detector. SEM was used to study the surface morphology of zeolite particles and NZ-nZVI. SEM analysis of samples was conducted at accelerating voltage within the 15–20 kV range, and a dwell time of 30 micro-seconds (µs) as reported in **Fig. 1**. The surface area is a critical factor in proper functioning of n-ZVI because the surface area is typically corresponding to the reactivity of n-ZVI particle, and the measured surface area of n-ZVI is between 8.4–46.27 m^2/g by $NaBH_4$ method [40]. Zeolite particles were quasi-spherical in shape with 2–30 µm particle size. The natural zeolite surface was comparatively smooth. The smaller particles were distributed all over the larger ones. Chain-Like structures were present in NZ-nZVI, which covered the zeolite grains [41]. After the utilization of NZ-nZVI particles in dye removal, they were filtered out and dried in the form of fragile chunks of iron. These NZ-nZVI chunk were found to be highly porous. Although impregnation of natural zeolite surface with nZVI significantly decreased the aggregation, some nanoparticles attraction persisted, as the presence of individual particle entities were slightly diminished. This existence in the form of an individual particle was seen again in the case of used NZ-nZVI particles. However, the surface of used NZ-nZVI was rougher as compared

to unloaded natural zeolite, due to buildup of iron oxides on the surface during the removal process [42].

The EDX detector results showed that the natural zeolite did not contain iron content, and it appeared after the loading of nZVI onto the natural zeolite surface as presented in **Fig. 2**. Iron was loaded in its nano zerovalent scale during the synthesis procedure. The loaded iron content was 9.5%, which is low as compared to most of the previously cited quantities in the literature [32, 43]**.** According to Luo et al. [32], the loaded iron content was 9.94% (w/w) in nZVI. The oxygen content increased only after use, which indicates the corrosion of NZ-nZVI particles. Synthesized NZ-nZVI contained sodium, which is expected to appear due to the use of $NaBH_4$ for reduction. The negligible sulfur contents were also detected, due to the use of sulfuric acid for pH control. Natural zeolite was free from sulfur as per EDX detection. No obvious peak of crystalline iron was noticed in the sample, which indicates the dispersion of iron species. These iron species formed very small-sized crystallites which were not detectable [32]. EDX detector was also used for the elemental composition of samples that are illustrated in Error! Reference source not found..

XRD Spectrum of natural zeolite is shown in **Fig. 3**. The XRD was used to investigate the mineralogical nature of the natural zeolite used as nZVI support. The characteristic strong peaks appeared at 13, 22.37, 26.6, 28.15, and 32 intensity in the spectrum indicate that the natural zeolite consists mostly of clinoptilolite [44]. It was observed that most of the peaks were fall in these three spectra, which indicate the presence of clinoptilolite, and model structural formula could be suggested as $(Na, K, Ca)_6(Si, Al)_{36}O_{72}\cdot 20H_2O$ [45]. The natural zeolite also contained heulandite confirmed by peaks appeared at 2theta values of 17.2, 26.6, and 35.86 in the spectra. The peak at

26.6 also shows the presence of quartz in the zeolite sample. A sufficient quantity of calcite was also observed at 3θ that is in agreement with the recently stated study [46]. In addition, the small quantity of phillipsite zeolite was also detected through its peaks appeared at 21.51 and 45.82 intensities [44]. Clinoptilolite is high silica-containing and one of the most common types of natural zeolite. It has a negatively charged surface, which tends to attract cations, such as Na^+.

FTIR spectra of natural zeolite and NZ-nZVI is represented in **Fig. 4**. The symmetric and asymmetric stretching of the hydroxyl group is shown by the peak at 3366.69 cm^{-1}. This is expected due to absorbed water present in the natural zeolite framework. The band at 1633 cm^{-1} represents the water molecularly bound within the zeolite structure, as well as the metal-O bonding. The aluminosilicate status of zeolite is evident from the peak at 1034 cm^{-1}, which is due to Al and/or Si bonding with oxygen. This is once again shown in the fingerprint region, where the peaks at 799.3 cm^{-1} and 780.59 cm^{-1} represent the Si-Al-O bonding. The results of natural zeolite spectrum are in good agreement with the previously reported IR studies [47, 48]. Ruiz-Baltazar and co-workers [47] stated that zeolite has a large surface area due to allotropic phase of SiO_2 that is recognized by the peak appeared at 797 cm^{-1} and is associated with O-Al and Si-O bonds, which are characteristically tectosilicates.

The FTIR spectrum of used NZ-nZVI was also recorded and is presented in **Fig. 4**. Some characteristic features of this spectrum are the significant increase in the depth of OH stretch band at 1330 cm^{-1} and the C-O stretch band at 1030 cm^{-1} that might be due to the ethanol used in the synthesis and storage process [49]. There is another shift in the spectrum, however, the direction of this shift is opposite in the fingerprint region at left half. Furthermore, the shift in OH stretch is

329 due to the loading of nZVI on the natural zeolite, which causes the IR to be absorbed at
330 comparatively lower frequencies. The stretching and bending vibrotational band of OH in water
331 molecule adsorbed over the n-ZVI surface was observed as 3422 and 1600 cm^{-1}, respectively [50].
332 Moreover, two new peaks appeared at 2884.6 cm^{-1} and 2823.37 cm^{-1} represent the OH bonding in
333 the iron oxide shell, most likely due to FeOOH.

334 ## 3.2 Aggregation reduction study of NZ-nZVI

335 Few batches of nZVI were also prepared to visually compare the aggregation behaviour of
336 supported and unsupported nZVI. The use of natural zeolite as support material for nZVI greatly
337 reduced nanoparticle aggregation. Some magnetic attraction existed between NZ-nZVI particles
338 which was trying to join with each other but were again separated by even very slight shear, while
339 the aggregated nZVI particles were able to resist even very vigorous mixing and therefore, had to
340 be ultrasonicated to separate [34]. Furthermore, the aggregation persisted even on vigorous manual
341 stirring. Aggregation dissipated when the liquid was subjected to ultrasonication for 20 min but
342 returned within 100 s when the ultrasonication was stopped. Therefore, once particles separated,
343 they aggregated immediately together. Natural zeolite supported nZVI demonstrated superior
344 dispersion in the aqueous media than their unsupported counterparts. The reduction in the
345 aggregation of nZVI by using support material is in agreement with several previously reported
346 studies [24, 51, 52]. Shahwan et al. [51] observed a partial reduction in the aggregation of iron
347 nanoparticles by intruding K10 as supporting material during the synthesis of nZVI particles.

3.3 Dye removal study

3.3.1 Removal of synthetic CI acid Orange 52 dye

Five different initial dye concentrations (5, 10, 15, 20, 25 mg/L) were used to check the synthetic Acid Orange 52 (AO52) dye removal over 180 min treatment. The results of different initial dye concentrations on synthetic AO52 dye removal are depicted in **Fig. 5**. Dye concentration drop over time, as well as an increase in percentage removal, was observed as illustrated in **Fig. 6**. The decrease in dye concentration over the treatment of 180 min was studied as a result of Fenton system comprising of NZ-nZVI/SPC. Furthermore, to remove dye from the aqueous solution the SPC and NZ-nZVI slurry were conveniently suspended in an aqueous matrix on slightest agitation that stayed in suspension for a considerable period due to negligible gravitational pull and small size of NZ-nZVI particles.

Moreover, visible decolourization of samples started after 10 min in all five concentrations (5, 10, 15, 20, 25 mg/L). Colour of the reaction mixture first turned from black to dark green tint and then to dark red/ brown after 29 min. The reaction mixture completely changed its colour after 70 min. The maximum rapid dye removal was observed within the first 10 min about 60% removal. Further, decolourization rate drops considerably after 20 min and maximum dye removal (>90%) was achieved after 180 min treatment at 15 mg/L concentration. More than 80% of dye removal was noted within 30 min of operation at 15 mg/L initial dye concentration. These findings correlate with the recently published research, which states 73.5% removal of atrazine by GO/nZVI within the first 30 of min treatment and the removal efficiency increased up to 81.6% with total elimination of atrazine after 240 min [53].

Dutta et al. [54] reported that more than 80% reduction of Remazol Brilliant Orange 3RID dye was achieved within the first 15 min treatment with nZVI catalyst. They also stated that one gram of nZVI significantly removed about 2207 mg of anthraquinone dye (RBMR) and 2757 mg of Remazol Brilliant Orange 3RID dye. With 5 mg/L concentration, 89.3% removal was recorded in the first 60 min. However, the following two hours resulted in only approximately 2.5% dye removal. The maximum dye removal was 93.5% in the case of 10 mg/L initial concentration and 94.8% in the case of 15 mg/L concentration after 180 min treatment as represented in **Fig. 7**. Comparable findings of a previous study stated that 96% decolourization of methyl orange dye was achieved while using CFA (coal fly ash) as supporting material for nanoscale ZVI through Fenton reaction at pH 3 [49].

A recent study reported about 80% removal of acid orange 7 (AO7) dye by using PMS/WMF as a supported carrier with Z-nZVI. But surprisingly after three-times regeneration of zeolite, the decolourization percentage of AO7 dye was improved and detected as 90% removal [34]. Similarly, a surprising rise in removal efficiency was observed at an initial dye concentration of 25 mg/L. Furthermore, 79.68 and 83.73% dye removal was recorded after 20 and 30 min of operation respectively at 25 mg/L concentration, as compared to 68.5 and 74.28% in the case of 20 mg/L concentration. Most probably the reason for this behaviour is the negative surface of clinoptilolite type natural zeolite used as NZ-nZVI support. Therefore, a 20 mg/L, the negative ions of dissociated AO52 are repelled due to similar charge of zeolite. However, when the initial concentration increases up to 25 mg/L the momentum of ions in motion overcomes the repelling effect of zeolite and adsorption of dye on NZ-nZVI and consequent removal performance

improves. These results are in agreement with the findings of several other researches, which reported remediation application of nZVI along with the advanced oxidation process [29, 55].

The overall dye removal percentage was decreased by increasing the an initial dye concentration above 15 mg/L such as the removal percentage decreased from 94.8 to 85.9% in the case of 25 mg/L concentration after 180 min treatment. This drop in the dye removal performance with respect to 15 mg/L concentration could be due to the high amount of dye molecules that are remediated by the same amount of NZ-nZVI and SPC dosage. These findings are also in agreement with those of Yang et al. [56], who stated a maximum 76.09% and minimum 41.74% removal of methyl orange dye (MO) by using S-nZVI/BC system at an initial dye concentration of 0.05 and 1 mM after 240 min treatment. Although this removal rate can be deemed satisfactory to current industrial practices when it comes to textile effluent decolourization, with the determination of optimum concentration of SPC. However, performance can be improved by using a smaller concentration amount and lesser treatment time [57].

3.3.2 Removal of actual dying effluents by NZ-nZVI/SPC Fenton system

Three different actual textile effluent samples including AEG, AEM and AEB (green, magenta and blended) were remediated by using NZ-nZVI/SPC Fenton system. Significant dye removal was achieved within 10 min of treatment. The dye removal efficiency was calculated from absorbances measured from the UV-vis spectrophotometer. Furthermore, the decrease in dye concentration was confirmed from UV-vis spectra. In the absorption spectra for AEG, the UV-vis spectras have been recorded from a wavelength range of 325–1000 nm using MAPADA V1100 Spectrophotometer. The highest peak in the pre-treatment spectra appears at 372 nm, which lies in the UV range. The bleaching, scouring, de-sizing, and mercerizing are the most significant pre-

treatments which are directly used before dying (after yarn) [57]. The significant peak in the visible range at 625 nm confirms the green colour of effluent as shown in **Fig. 8.** The unusual high peak in UV range is due to the presence of several compounds in affluent, especially glacial acetic acid. The post-treatment spectra showed a decrease in absorption across the spectral range. The peak representing the green colour (pre-treatment) is completely flattened, indicating significant green chromophore removal. Mao and his research group suggested that 98.5% reduction of malachite green (MG) effluent was achieved from the textile dyeing solution by using microwave/nZVI with 16 mL/min influent flow rate [58].

Fenton system can mineralize the acetic acid, which is also evident from a decrease in UV region peak height after treatment with NZ-nZVI/SPC system. Similar dye removal behaviour is also observed in the case of AEM as presented in **Fig. 9**. The peak at 540 nm represents the characteristic for a violet/magenta coloured liquid in the pretreatment spectra, while a similar decrease in UV range peak was observed in post-treatment spectra. These results are correlated with the findings of Kecic et al. [37] who reported that 84.06% reduction of Magenta colour from aqueous solution after 60 min treatment with oak leave nano-zerovalent iron (OAK-nZVI). They also stated that the destruction of azo bond in chromophore is responsible for the decolourization of dye solution. Therefore, to eliminate the effect of dilution the spectra was reproduced after removal of 50% solvent.

The dye removal in blended effluent (AEB) was also studied by utilizing UV-vis spectra, due to its comparatively simpler composition. In those cases where effluent is complex containing a large number of different chromophores or other additives, then spectrophotometric determination

becomes unreliable and therefore techniques are recommended. In the pretreatment spectra, visible peak appeared at 625 nm, while the UV range peak appeared at 358 nm. These results are represented in **Fig. 10**. The NZ-nZVI system was also able to successfully remove dye from AEB sample because of the flattening of visible spectrum peak. Similar findings that are reported in the literature in agreement with the obtained results [59, 60]. Nidhi et al. [59] observed that 72.7% decolourization of the actual untreated filtered wastewater by using resin-supported nZVI.

Surprisingly, the colour removal percentage decreased (72.7–67.3%) by increasing the solution volume from 100 to 2600 mL. This could be because of unknown chemicals and auxiliaries in the actual effluent. Similarly, another study reported that nZVI effectively removed the colour of azo dye by breaking the azo linkage and generated free Fe^{2+} ions. This Fe^{2+} reacts with H_2O_2 through Fenton oxidation and subsequently removed up to 67% of colour from azo dye with 125 mg/L dose of nZVI [60]. Moreover, Fenton reactions provided dual function at a time including coagulation and oxidation that significantly helped out in the decolorization of textile wastewater [61].

4 Conclusions

The present study aimed to analyze textile dye removal potential of nZVI supported on natural zeolite in a Fenton like system for the activation of sodium percarbonate (SPC), which served as a source of hydroxyl radical generation. There was a significant reduction in the characteristic aggregation behaviour, with the particles being efficiently distributed in aqueous media. Whereas in previous literature, NZ-nZVI was filtered and dried in vacuum/nitrogen environment due to its rapidly corroding tendency. NZ-nZVI was used as a slurry with dilute 70% ethanol solution that served as an aqueous media of storage and transportation. The same method was utilized for the

462 removal of dye from undiluted and unfiltered actual effluent, which showed effective
463 decolorization within 30 min treatment. Both actual effluent and synthetic textile effluent were
464 decolorized by using NZ-nZVI/SPC catalyst. A maximum 94.86% decolorization of Acid Orange
465 52 (an azo dye) dye was achieved at 15 mg/L concentration after 180 min treatment. Moreover,
466 NZ-nZVI nanoparticles were also significantly removed from the actual textile effluent (AEG,
467 AEM, and AEB), as quantified by UV-vis absorption spectra. Owing to cheap, safer reagent, high
468 biodegradability, and significant decolorization potential within a short time the NZ-nZVI/SPC
469 system is recommended to be practically feasible for industrial effluent, ground and surface water
470 treatment. The output of nZVI/Fenton/SBH system can be fed into the conventional biological
471 treatment process to further polish the effluent being treated. Furthermore, borohydride synthesis
472 method results in the evolution of hydrogen gas, there are lack of studies to determine the potential
473 of this hydrogen gas as a possible energy source. Therefore, more studies are recommended to be
474 conducted to use this hydrogen gas for possible positive purposes. Moreover, nZVI in combination
475 with other processes such as photolysis, ozonation or ultrasonication could be an innovative option
476 to treat wastewater.

477 # Acknowledgement

478 The authors are grateful for the financial support from Higher Education Commission of Pakistan,
479 under startup research grant programme (SRGP) project # 1530.

480

References

1. Mani, S., P. Chowdhary, and R.N. Bharagava, Textile wastewater dyes: toxicity profile and treatment approaches, in Emerging and Eco-Friendly Approaches for Waste Management. 2019, Springer. p. 219-244.
2. Sher, F., et al., Implications of advanced wastewater treatment: Electrocoagulation and electroflocculation of effluent discharged from a wastewater treatment plant. Journal of Water Process Engineering, 2020. 33: p. 101101.
3. Sharma, A.K., et al., GHG mitigation potential of solar industrial process heating in producing cotton based textiles in India. Journal of Cleaner Production, 2017. 145: p. 74-84.
4. Chowdhary, P., A. Raj, and R.N. Bharagava, Environmental pollution and health hazards from distillery wastewater and treatment approaches to combat the environmental threats: a review. Chemosphere, 2018. 194: p. 229-246.
5. Burkinshaw, S.M. and G. Salihu, The role of auxiliaries in the immersion dyeing of textile fibres: Part 1 an overview. Dyes and Pigments, 2019. 161: p. 519-530.
6. Chequer, F.D., et al., Textile dyes: dyeing process and environmental impact. Eco-friendly textile dyeing finishing, 2013. 6: p. 151-176.
7. Franca, R.D., et al., Biodegradation Products of a Sulfonated Azo Dye in Aerobic Granular Sludge Sequencing Batch Reactors Treating Simulated Textile Wastewater. ACS Sustainable Chemistry Engineering, 2019. 7(17): p. 14697-14706.
8. Zarren, G., B. Nisar, and F. Sher, Synthesis of anthraquinone based electroactive polymers: A critical review. Materials Today Sustainability, 2019: p. 100019.
9. Sharma, V.K. and M. Feng, Water depollution using metal-organic frameworks-catalyzed advanced oxidation processes: a review. Journal of hazardous materials, 2019. 372: p. 3-16.
10. Shah, M.P., Bioremediation of Azo Dye, in Microbial Wastewater Treatment. 2019, Elsevier. p. 103-126.
11. Yusuf, M., Synthetic dyes: a threat to the environment and water ecosystem. Textiles Clothing, 2019: p. 11-26.
12. Fradj, A.B., et al., Removal of azoic dyes from aqueous solutions by chitosan enhanced ultrafiltration. Results in Chemistry, 2020. 2: p. 100017.
13. Sher, F., A. Malik, and H. Liu, Industrial polymer effluent treatment by chemical coagulation and flocculation. Journal of Environmental Chemical Engineering, 2013. 1(4): p. 684-689.
14. Güleç, F., F. Sher, and A. Karaduman, Catalytic performance of Cu-and Zr-modified beta zeolite catalysts in the methylation of 2-methylnaphthalene. Petroleum Science, 2019. 16(1): p. 161-172.
15. Sun, Y., et al., Combination of plasma oxidation process with microbial fuel cell for mineralizing methylene blue with high energy efficiency. Journal of Hazardous Materials, 2020. 384: p. 121307.
16. Sharma, V.K., J. Zhao, and H. Hidaka, Mechanism of photocatalytic oxidation of amino acids: Hammett correlations. Catalysis Today, 2014. 224: p. 263-268.
17. Ganzenko, O., et al., Bioelectro-Fenton: evaluation of a combined biological—advanced oxidation treatment for pharmaceutical wastewater. Environmental Science Pollution Research, 2018. 25(21): p. 20283-20292.

18. Danish, M., et al., An efficient catalytic degradation of trichloroethene in a percarbonate system catalyzed by ultra-fine heterogeneous zeolite supported zero valent iron-nickel bimetallic composite. Applied Catalysis A: General, 2017. 531: p. 177-186.
19. Garcia-Segura, S. and E. Brillas, Applied photoelectrocatalysis on the degradation of organic pollutants in wastewaters. Journal of Photochemistry Photobiology C: Photochemistry Reviews, 2017. 31: p. 1-35.
20. Carbajo, J., et al., Study of application of titania catalysts on solar photocatalysis: Influence of type of pollutants and water matrices. Chemical Engineering Journal, 2016. 291: p. 64-73.
21. Raman, C.D. and S. Kanmani, Textile dye degradation using nano zero valent iron: a review. Journal of Environmental Management, 2016. 177: p. 341-355.
22. Shih, Y.-H., C.-P. Tso, and L.-Y. Tung, Rapid degradation of Methyl Orange with nanoscale zervalent iron particles. Environmental Engineering and Management Journal, 2010. 20(3): p. 130-143.
23. Yan, W., et al., Iron nanoparticles for environmental clean-up: recent developments and future outlook. Environmental Science: Processes Impacts, 2013. 15(1): p. 63-77.
24. Liu, F., et al., Graphene-supported nanoscale zero-valent iron: removal of phosphorus from aqueous solution and mechanistic study. Journal of Environmental Sciences, 2014. 26(8): p. 1751-1762.
25. Stefaniuk, M., P. Oleszczuk, and Y.S. Ok, Review on nano zerovalent iron (nZVI): from synthesis to environmental applications. Chemical Engineering Journal, 2016. 287: p. 618-632.
26. Shi, X., et al., Optimizing the removal of rhodamine B in aqueous solutions by reduced graphene oxide-supported nanoscale zerovalent iron (nZVI/rGO) using an artificial neural network-genetic algorithm (ANN-GA). Nanomaterials, 2017. 7(6): p. 134.
27. Han, L., et al., Biochar supported nanoscale iron particles for the efficient removal of methyl orange dye in aqueous solutions. PloS one, 2015. 10(7).
28. Jin, X., et al., Synthesis of kaolin supported nanoscale zero-valent iron and its degradation mechanism of Direct Fast Black G in aqueous solution. Materials Research Bulletin, 2015. 61: p. 433-438.
29. Kerkez, D.V., et al., Three different clay-supported nanoscale zero-valent iron materials for industrial azo dye degradation: A comparative study. Journal of the Taiwan Institute of Chemical Engineers, 2014. 45(5): p. 2451-2461.
30. Malik, S.N., et al., Catalytic ozone pretreatment of complex textile effluent using Fe2+ and zero valent iron nanoparticles. Journal of hazardous materials, 2018. 357: p. 363-375.
31. Dutta, S., et al., Modified synthesis of nanoscale zero-valent iron and its ultrasound-assisted reactivity study on a reactive dye and textile industry effluents. Desalination Water Treatment, 2016. 57(41): p. 19321-19332.
32. Luo, S., et al., Synthesis of reactive nanoscale zero valent iron using rectorite supports and its application for Orange II removal. Chemical Engineering Journal, 2013. 223: p. 1-7.
33. Lien, H.-L., et al., Recent progress in zero-valent iron nanoparticles for groundwater remediation. Journal of Environmental Engineering Management, 2006. 16(6): p. 371.
34. Fu, X., et al., Enhanced peroxymonosulfate activation by coupling zeolite-supported nano-zero-valent iron with weak magnetic field. Separation Purification Technology, 2020. 230: p. 115886.

35. Jafarnia, M.S., M.K. Saryazdi, and S.M. Moshtaghioun, Use of bacteria for repairing cracks and improving properties of concrete containing limestone powder and natural zeolite. Construction Building Materials, 2020. 242: p. 118059.
36. Satapanajaru, T., et al., Enhancing decolorization of Reactive Black 5 and Reactive Red 198 during nano zerovalent iron treatment. Desalination, 2011. 266(1-3): p. 218-230.
37. Kecić, V., et al., Optimization of azo printing dye removal with oak leaves-nZVI/H2O2 system using statistically designed experiment. Journal of Cleaner Production, 2018. 202: p. 65-80.
38. Deniz, F. and S. Saygideger, Equilibrium, kinetic and thermodynamic studies of Acid Orange 52 dye biosorption by Paulownia tomentosa Steud. leaf powder as a low-cost natural biosorbent. Bioresource technology, 2010. 101(14): p. 5137-5143.
39. Maučec, D., et al., Titania versus zinc oxide nanoparticles on mesoporous silica supports as photocatalysts for removal of dyes from wastewater at neutral pH. Catalysis Today, 2018. 310: p. 32-41.
40. Hwang, Y.-H., D.-G. Kim, and H.-S. Shin, Effects of synthesis conditions on the characteristics and reactivity of nano scale zero valent iron. Applied Catalysis B: Environmental, 2011. 105(1-2): p. 144-150.
41. Bae, S. and W. Lee, Inhibition of nZVI reactivity by magnetite during the reductive degradation of 1, 1, 1-TCA in nZVI/magnetite suspension. Applied Catalysis B: Environmental, 2010. 96(1-2): p. 10-17.
42. Bae, S., et al., Effect of NaBH4 on properties of nanoscale zero-valent iron and its catalytic activity for reduction of p-nitrophenol. Applied Catalysis B: Environmental, 2016. 182: p. 541-549.
43. Danish, M., et al., Degradation of chlorinated organic solvents in aqueous percarbonate system using zeolite supported nano zero valent iron (Z-nZVI) composite. Environmental science pollution research, 2016. 23(13): p. 13298-13307.
44. Abukhadra, M.R. and A.S. Mohamed, Adsorption removal of safranin dye contaminants from water using various types of natural zeolite. Silicon, 2019. 11(3): p. 1635-1647.
45. Mirzaei, H., et al., Plasma modification of a natural zeolite to improve its adsorption capacity of strontium ions from water samples. International Journal of Environmental Science Technology, 2019. 16(10): p. 6157-6166.
46. Wahono, S.K., et al., Physico-chemical modification of natural mordenite-clinoptilolite zeolites and their enhanced CO2 adsorption capacity. Microporous Mesoporous Materials, 2020. 294: p. 109871.
47. Ruíz-Baltazar, A., et al., Preparation and characterization of natural zeolite modified with iron nanoparticles. Journal of Nanomaterials, 2015. 2015.
48. Bakatula, E.N., A.K. Mosai, and H. Tutu, Removal of uranium from aqueous solutions using ammonium-modified zeolite. South African Journal of Chemistry, 2015. 68(1): p. 165-171.
49. Yoon, S. and S. Bae, Novel synthesis of nanoscale zerovalent iron from coal fly ash and its application in oxidative degradation of methyl orange by Fenton reaction. Journal of hazardous materials, 2019. 365: p. 751-758.
50. Bagbi, Y., et al., Nanoscale zero-valent iron for aqueous lead removal. Adv. Mater. Proc., 2017.
51. Shahwan, T., et al., Synthesis and characterization of bentonite/iron nanoparticles and their application as adsorbent of cobalt ions. Applied Clay Science, 2010. 47(3-4): p. 257-262.

52. Tesh, S.J. and T.B. Scott, Nano-composites for water remediation: A review. Advanced Materials, 2014. 26(35): p. 6056-6068.
53. Xing, R., et al., Graphene oxide-supported nanoscale zero-valent iron composites for the removal of atrazine from aqueous solution. Colloids Surfaces A: Physicochemical Engineering Aspects, 2020: p. 124466.
54. Dutta, S., et al., Rapid reductive degradation of azo and anthraquinone dyes by nanoscale zero-valent iron. Environmental Technology Innovation, 2016. 5: p. 176-187.
55. Shih, Y.-H. and C.-P. Tso, Fast decolorization of azo-dye congo red with zerovalent iron nanoparticles and sequential mineralization with a fenton reaction. Environmental Engineering Science, 2012. 29(10): p. 929-933.
56. Yang, L., et al., Removal of Methyl Orange from Water Using Sulfur-Modified nZVI Supported on Biochar Composite. Water, Air, Soil Pollution, 2018. 229(11): p. 355.
57. Paździor, K., L. Bilińska, and S. Ledakowicz, A review of the existing and emerging technologies in the combination of AOPs and biological processes in industrial textile wastewater treatment. Chemical Engineering Journal, 2019. 376: p. 120597.
58. Mao, Y., J. Xu, and C. Ma, A continuous microwave/nZVI treatment system for malachite green removal: system setup and parameter optimization. Desalination Water Treatment, 2016. 57(51): p. 24395-24405.
59. Ahuja, N., A.K. Chopra, and A.A. Ansari, Textile dye removal using nZVI particles supported on cation exchange resin. Int. J. Chemtech. Res., 2017. 10(5): p. 858-866.
60. Yu, R.-F., et al., Monitoring of ORP, pH and DO in heterogeneous Fenton oxidation using nZVI as a catalyst for the treatment of azo-dye textile wastewater. Journal of the Taiwan Institute of Chemical Engineers, 2014. 45(3): p. 947-954.
61. Yu, R.F., et al., Control of the Fenton process for textile wastewater treatment using artificial neural networks. Journal of Chemical Technology Biotechnology, 2010. 85(2): p. 267-278.

List of Tables

Table 1. The elemental compositions of natural zeolite, NZ-nZVI, and spent NZ-nZVI for synthetic CI acid orange 52 dye removal by EDX.

Element	Natural Zeolite (%)	NZ-nZVI (%)	Spent NZ-nZVI (%)
Si	24.34	1.11	13.48
Al	5.23	23.98	3.12
O	67.64	59.40	68.45
Mg	1.10	0.00	0.55
K	0.64	-	-
Ca	1.05	-	0.95
Fe	0.00	1.38	9.50
Na	0.00	11.96	2.72
S	0.00	0.86	-

List of Figures

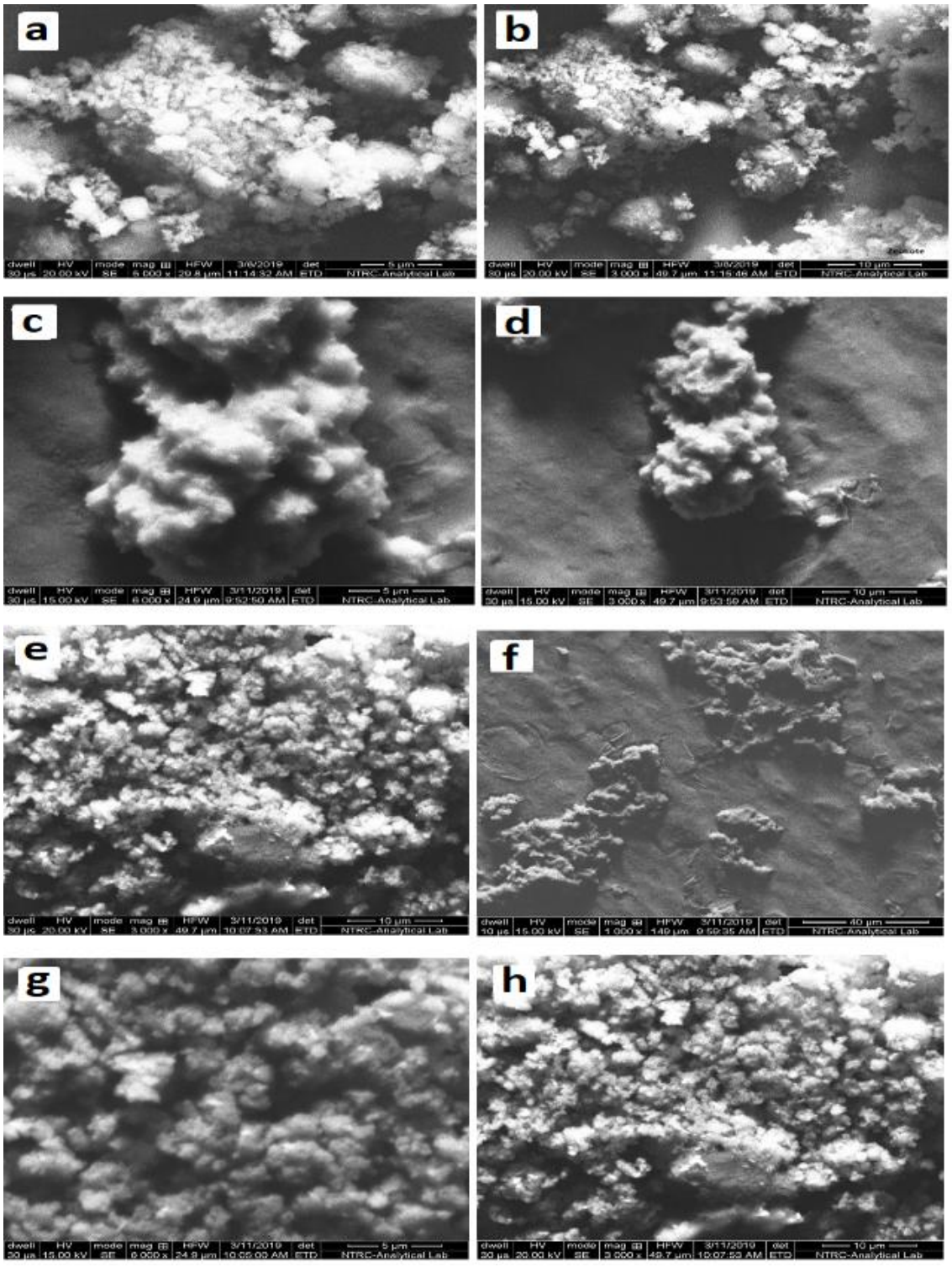

Fig. 1. SEM analysis of natural zeolite (a and b), NZ-nZVI (c, d, e, and f), and spend NZ-nZVI (g and h) composites onto synthetic CI acid orange 52 dye removal.

654

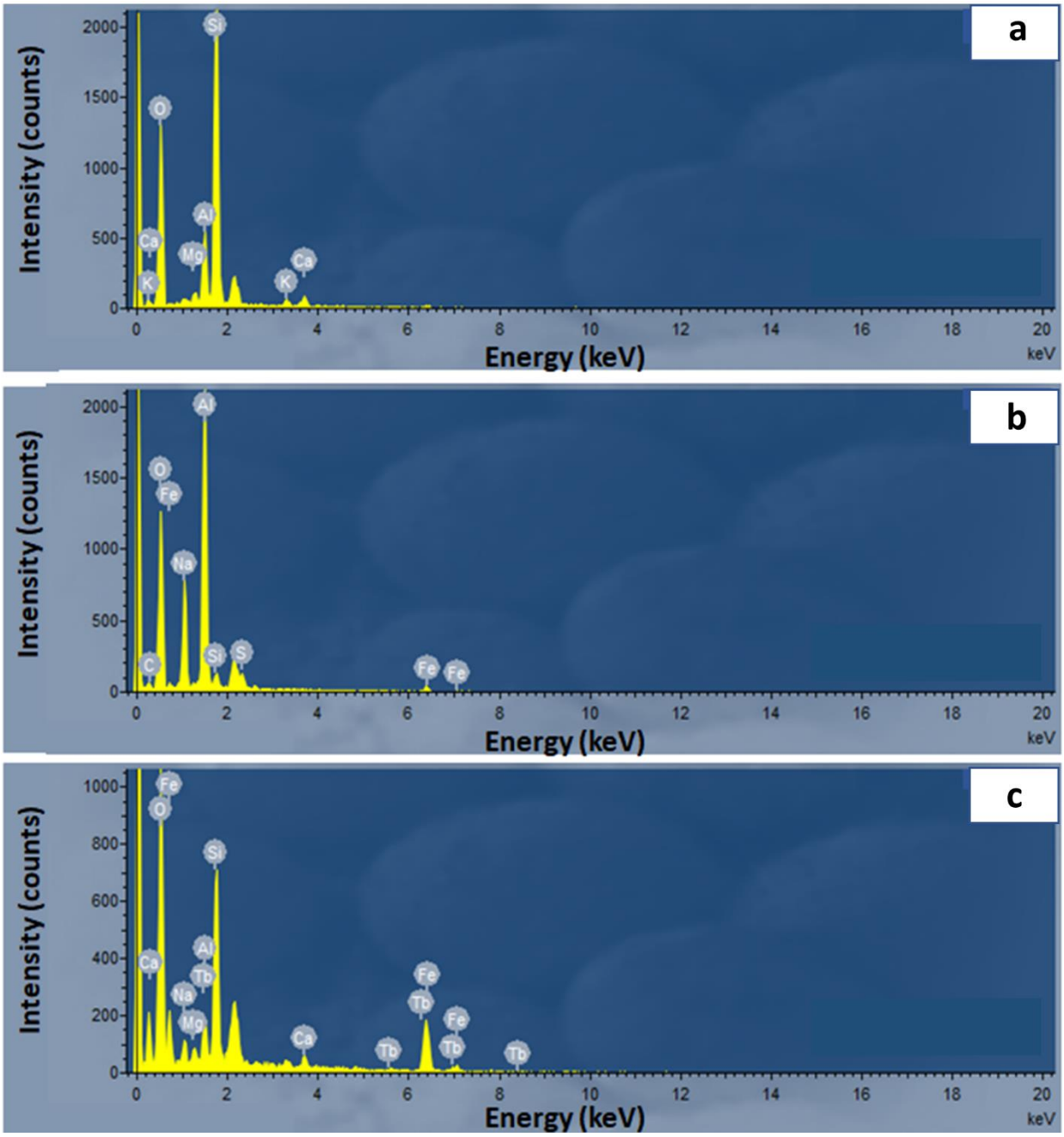

655

656 **Fig. 2.** EDX spectrum of **(a)** natural zeolite, **(b)** NZ-nZVI, and **(c)** spent NZ-nZVI composites for
657 CI acid orange 52 dye removal.

658

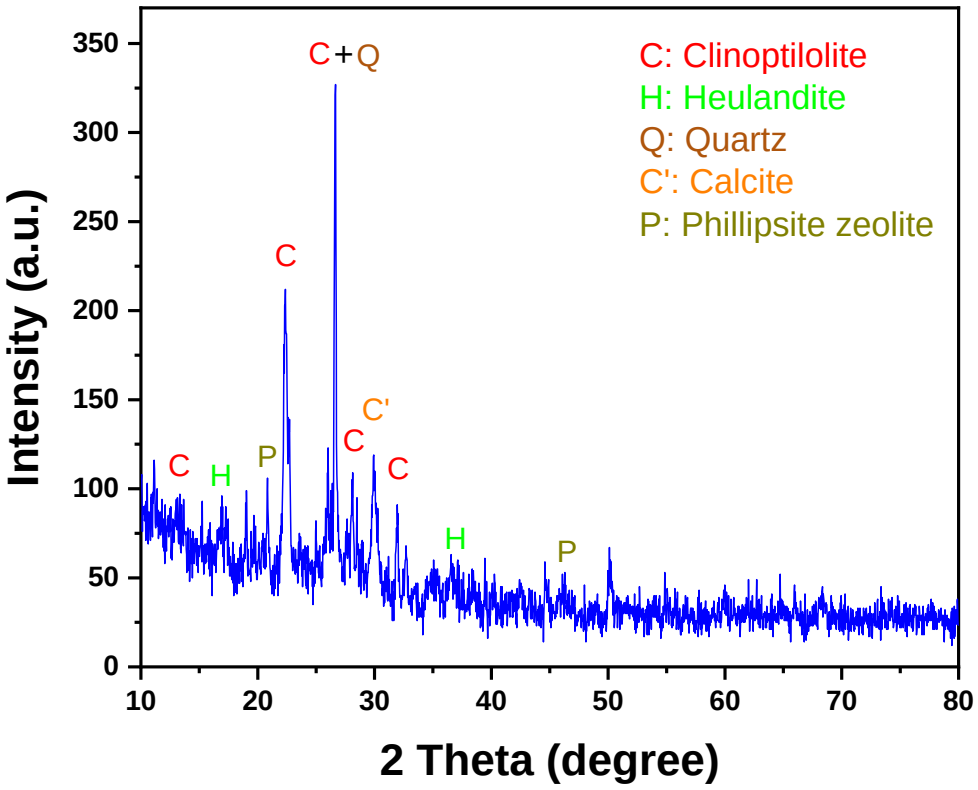

659

660 **Fig. 3.** XRD spectrum of natural zeolite for the determination of its composition as support
661 material of nZVI.

662

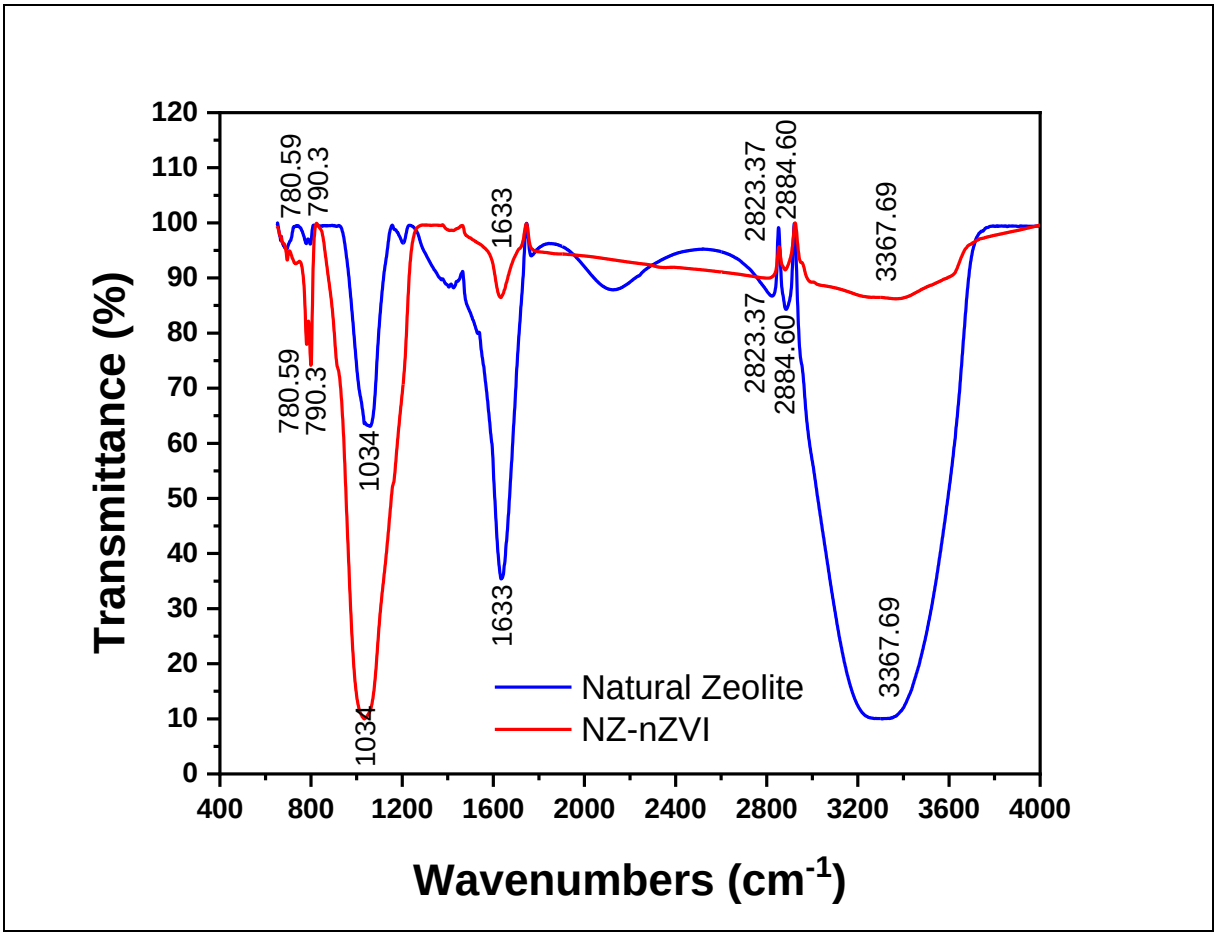

Fig. 4. FTIR spectra of AO52 dye removal by natural zeolite and NZ-nZVI composites.

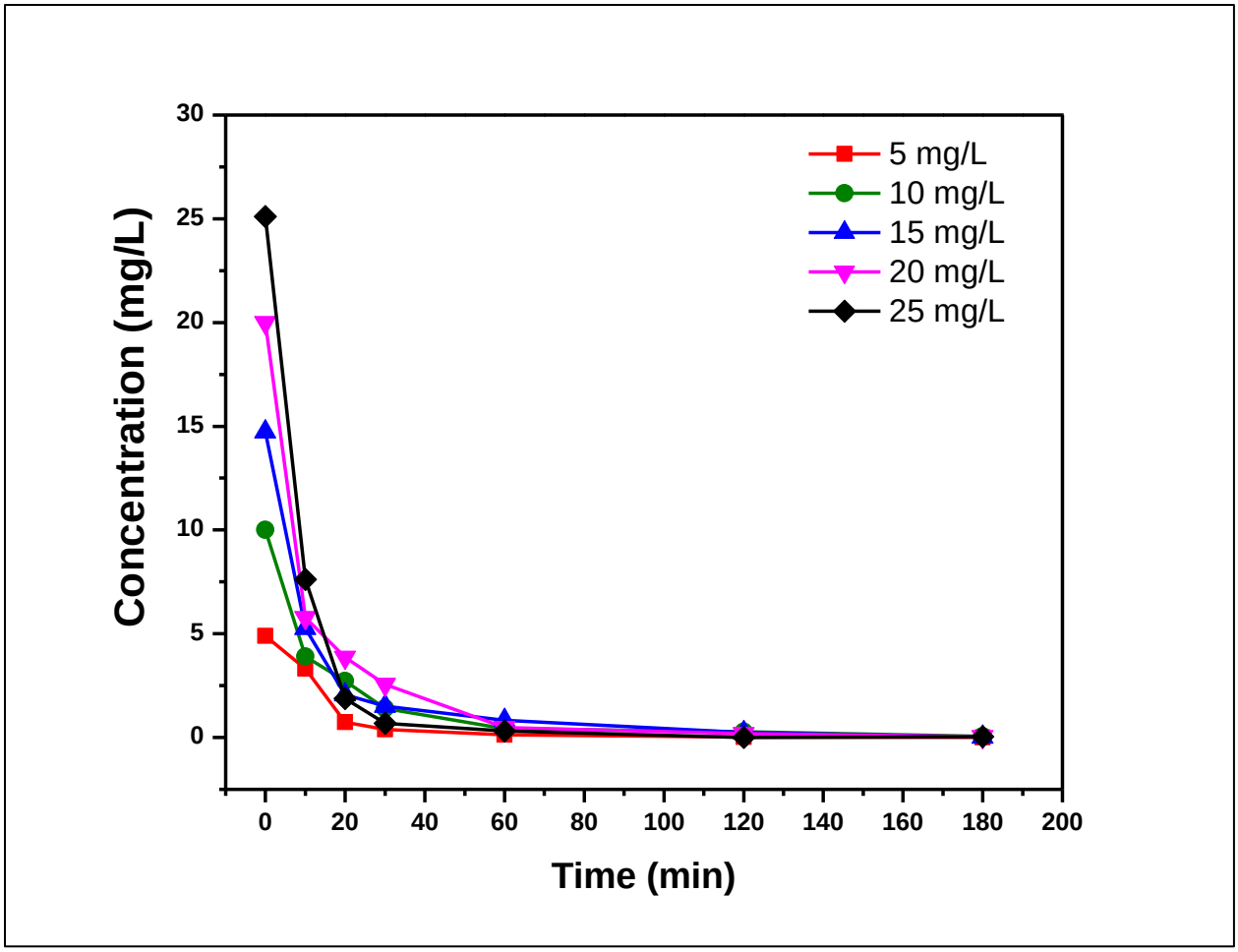

Fig. 5. The removal efficiency of OA52 dye by continuous NZ-nZVI treatment for 180 min at different dye concentrations and neutral pH.

674

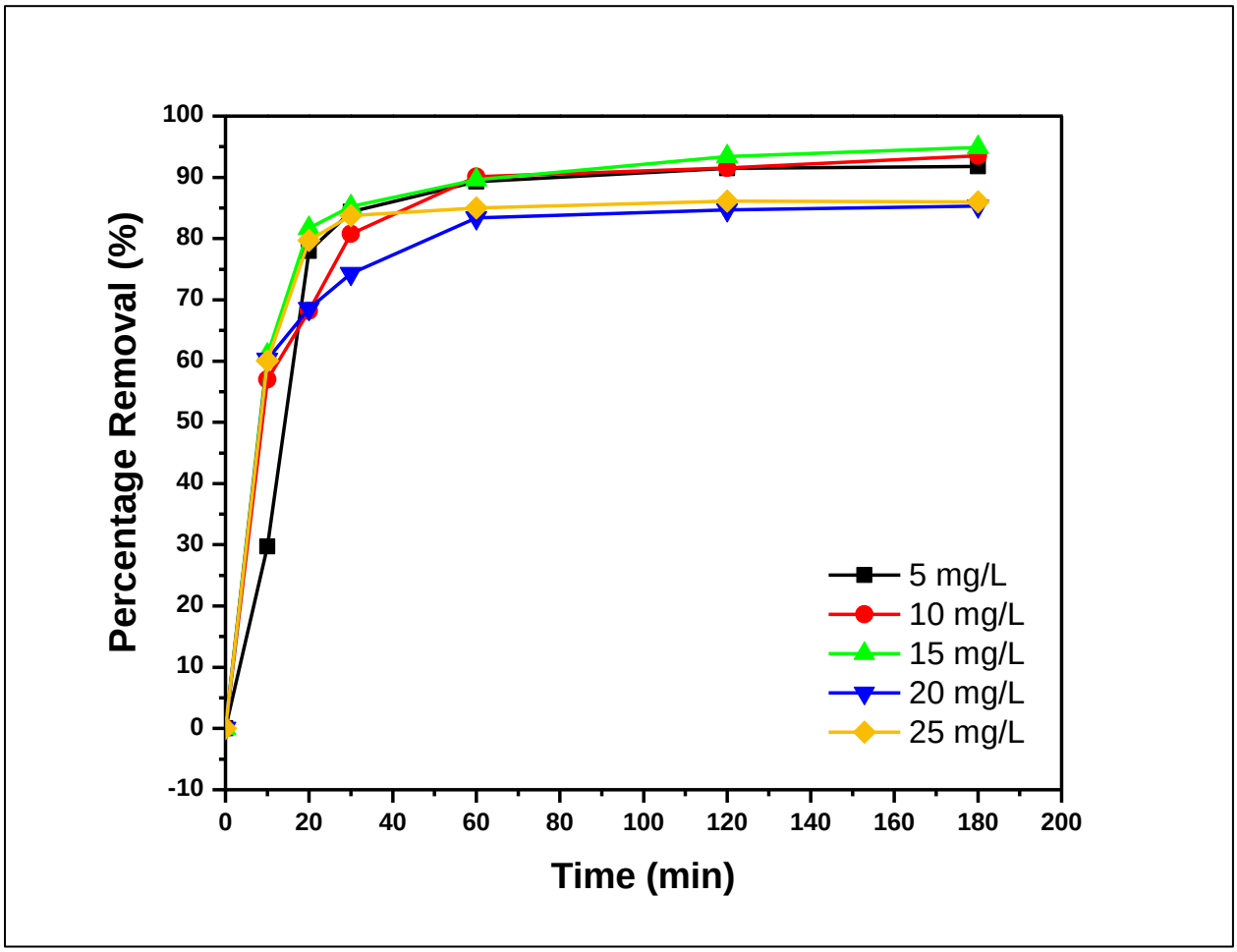

675

676 **Fig. 6.** The effect of time on the percentage removal of synthetic CI acid orange 52 dye at neutral
677 pH after 180 min treatment.

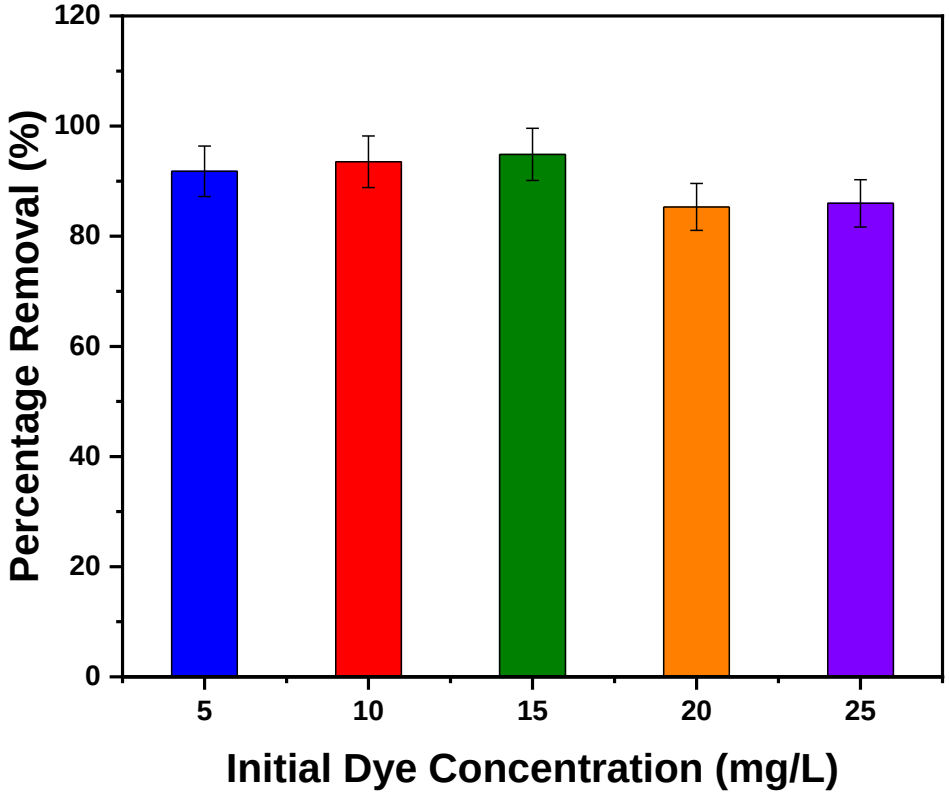

678

679 **Fig. 7.** Effect of initial dye concentration on percentage removal of synthetic CI acid orange 52
680 dye after 180 min treatment.

681

682

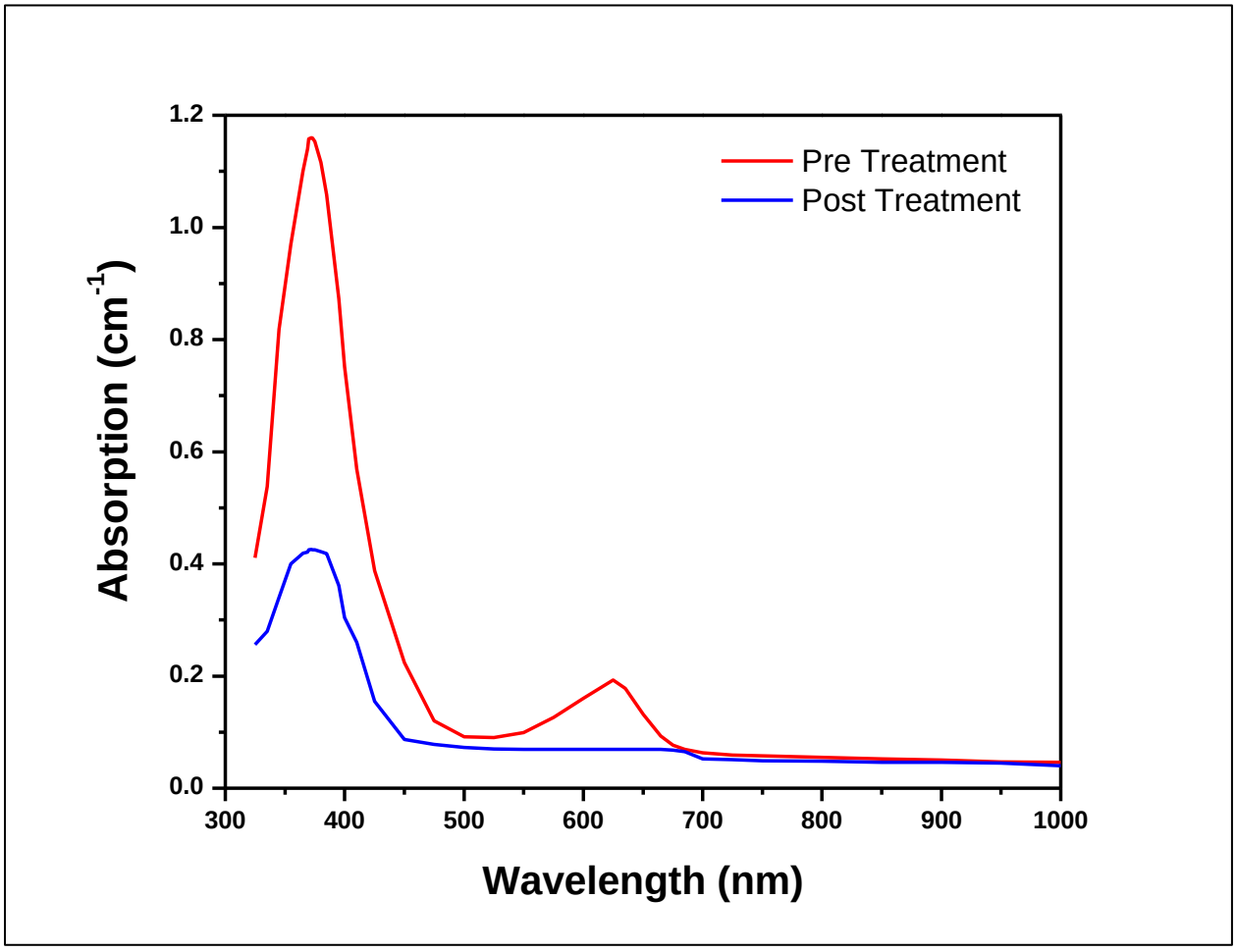

683

684 **Fig. 8.** The pre and post-treatment of actual effluent green (AEG) colour by NZ-nZVI composite.

685

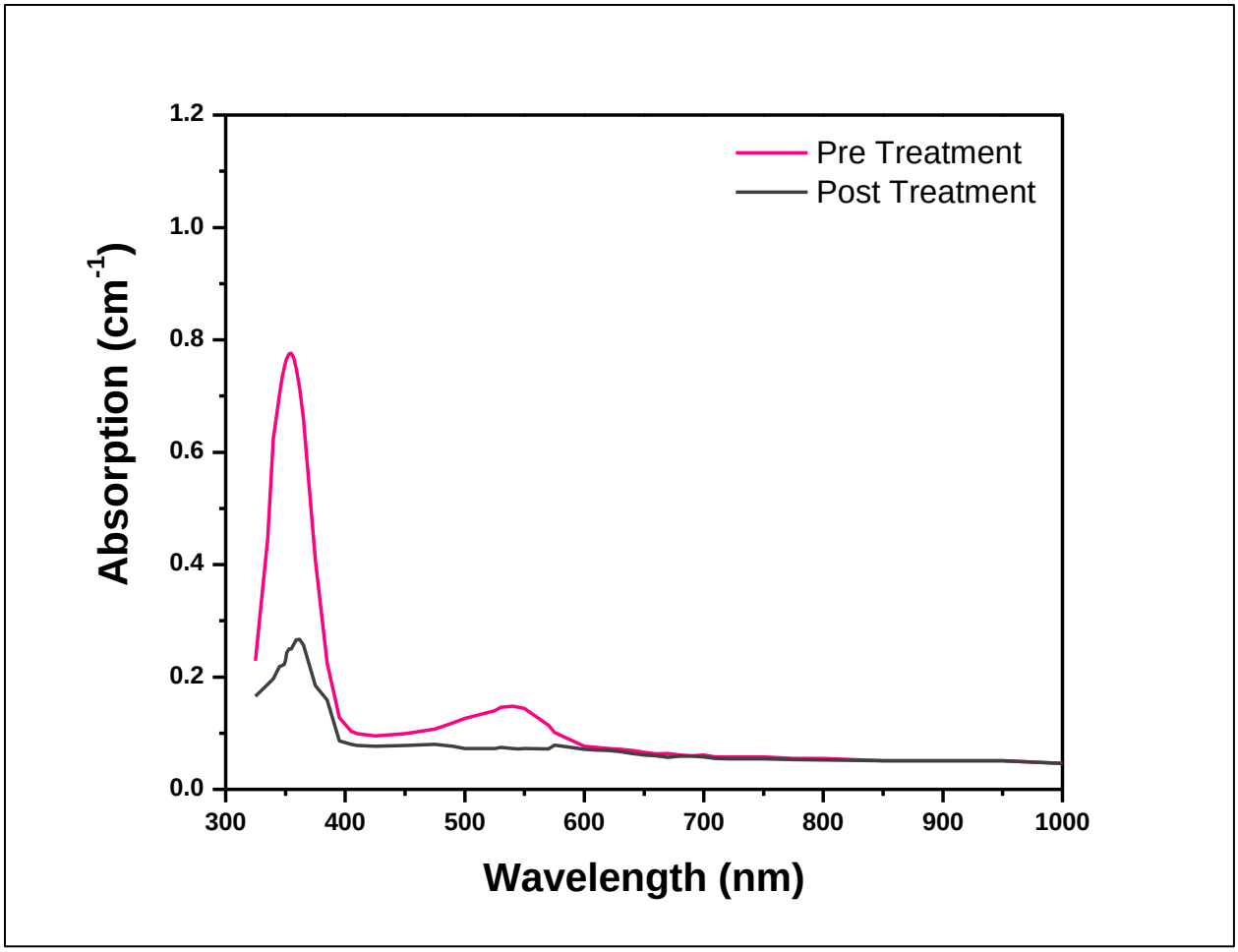

686

687 **Fig. 9.** The effect of pre and post-treatment on the removal of actual effluent magenta (AEM)
688 colour by natural zeolite modified nZVI.

689

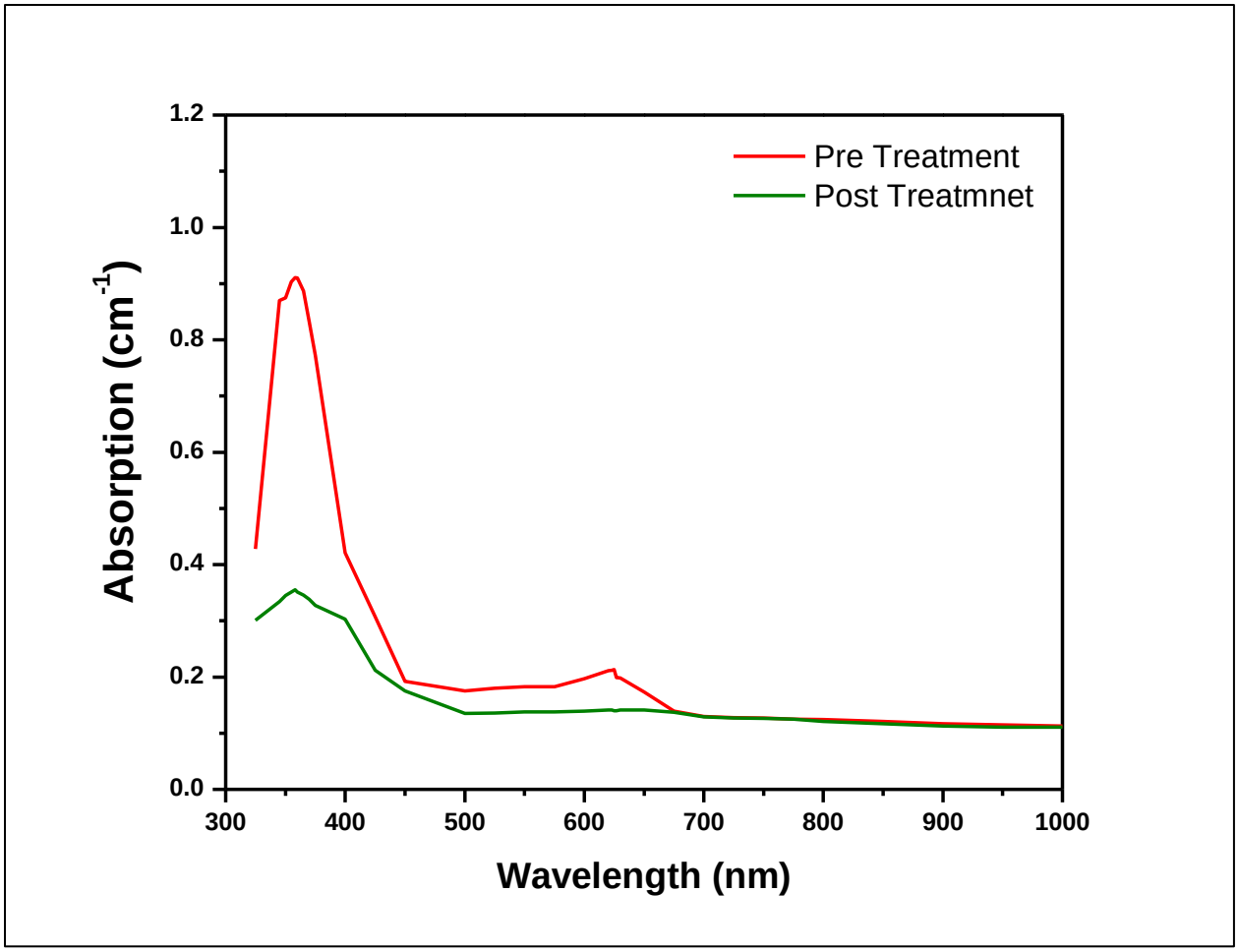

690

691 **Fig. 10**. Spectrophotometer analysis of pre and post-treatment of AEB colour removal by natural
692 zeolite modified nZVI.

693

Graphical Abstract